An Image-Carrying Fiber Optic Probe to Investigate Solids Distribution Around an Immersed Surface in a Gas-Fluidized Bed

S. C. Saxena, D. C. Patel, D. Kathuria
Department of Chemical Engineering
University of Illinois
Chicago, IL 60680

Introduction

A number of experimental techniques such as photographic, X-ray, capacitance, and electroresistivity probes have been employed to investigate the dynamics of gas-solid fluidized beds. Detailed knowledge of hydrodynamic behavior is essential to interpret and predict heat and mass transfer and solids elutriation from such systems. Saxena et al. (1984), Werther and Molerus (1973), and others have pointed out that in general these techniques do not provide a unique approach to probe the interior of a two-phase reactor. In recent years fiber optic probes have been developed, but only a few investigations using such probes have appeared so far. We briefly mention these efforts and report an investigation dealing with solids distribution around the circumference of a horizontal tube in a gas-fluidized bed using a novel image-carrying fiber optic probe.

A fiber optic probe operates on the principle of total internal reflection and is therefore sensitive to the changes of the medium refractive index present at its tip (Kapany, 1967). Ishida and coworkers have used multifiber reflective probes to measure particle velocities, bubble sizes, and bubble velocities in a three-dimensional gas-fluidized bed. Light was sent from the central fiber and was received from the peripheral fibers after reflection from the particle surface. Two probes arranged one above the other and separated by a known distance enabled determination of bubble velocity (Ishida et al., 1980). The bubble diameter was determined by an assembly of eight fiber-bundle probes (Ishida and Hatano, 1984). The light signal received by each fiber was converted to an electrical signal by a phototransistor and registered on a data recorder. Louis (1982) has also reported preliminary measurements with a quartz fiber probe in a fluidized-bed combustor. Peters et al. (1983) have used an image-carrying probe to study the particle ejection velocity at the top surface of a gas-fluidized bed. The bed surface was illuminated by external lights and the input end of the probe was positioned at the center, just above the bed surface, where bubbles were ejected. The image of the erupting bubbles was transported to the output end of the probe and was recorded by a high-speed camera. This work is different from others in that the optical signal was not converted to an electrical signal for detection, but instead the optical image was directly recorded on photographic film. However, such a probe cannot be employed to investigate the interior of a bed. Fiber optic probes have also been used to study gas-liquid and gas-liquid-solid systems, but these are not referenced in the present work, which is confined to gas-solid systems.

Experimental

The fluidized-bed facility together with the associated equipment utilized in the present investigation is described in detail by Verma and Saxena (1983), hence only the major relevant features and modifications are briefly mentioned here. The fluidizing air is supplied by two 18.65 kW air-cooled compressors, capable of delivering a total of 0.1 m^3/s of air at 377 kPa. The compressed air is dried, filtered to remove water and oil vapors, and metered on rotameters before entering the fluidized-bed system. The square cross section fluidization column is 0.305 m to a side, and consists of a plenum chamber, a bubble-cap distributor plate, and test and freeboard sections. The test section is 0.61 m tall and is provided with a front Plexiglas window for visual observations. Two Plexiglas side plates are used to mount a 10 mm ID glass tube of 0.5 mm wall thickness carrying an inserted fiber optic probe (A. O. Scientific Instruments); details of this borescope are given below. As bed material spherical glass beads of a narrow size range, 1.2 to 1.7 mm, with an average diameter d_p of 1.4 mm are used. To determine the mean bed voidage, 6.4 mm copper pressure probes mounted flush with the bed walls and connected to liquid manometers are employed. The off-gas from the column passes through primary and secondary cyclones and then through a cloth filter before venting into the exhaust duct.

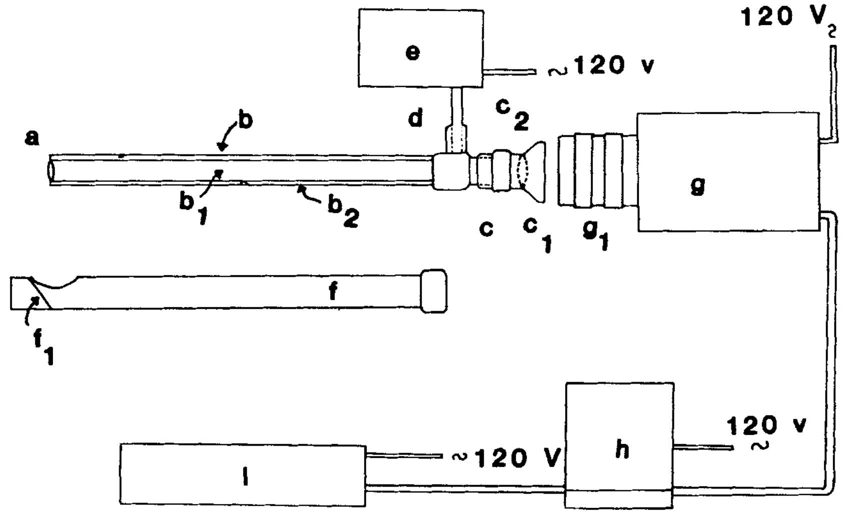

Figure 1. Borescope and associated measuring equipment.

a. Objective lens
b. Transmitting part
b_1. Image guide
b_2. Light guide
c. Eyepiece assembly
c_1. Relay lens
c_2. Slide focus control
d. Light guide input adaptor
e. Light source
f. Stainless steel tube
f_1. Right-angle mirror
g. TV camera
g_1. C-mount lens
h. TV monitor
i. Industrial VCR

A diagram of the borescope is shown in Figure 1. The scope consists of an objective lens *a*, a transmitting part *b*, and an eyepiece assembly *c*. The transmitting part comprises an inner image guide, b_1, prepared by bundling together parallel glass fibers of 30 μm dia., and an outer light guide, b_2, made from similar fibers to illuminate the object to be viewed. The light guide is enclosed in a 8 mm stainless steel tube. The right end of the transmitting part in the diagram is referred to as the proximal end; here the light-carrying fibers communicate to the external light source *e* through a light guide input adaptor *d*. The left end of the transmitting part is called the distal end; here the objective lens *a* with a field of view of 45° is attached to the image guide. At the proximal end of the image guide is the eyepiece assembly *c*, comprising a relay lens, c_1, and a slide focus control, c_2. The overall length of the borescope is 30 cm and the optical system has a depth of field varying from 1 mm to infinity. The forward viewing is conveniently converted for right-angle observation by slipping a stainless steel tube, *f*, with right-angle mirror f_1 over the transmitting part, *b*. 360° rotation of the tube *f* containing the right-angle mirror allows quick and effortless viewing around the circumference of the glass tube. The external light source *e* with variable light intensity capability (50, 100, 150 W) is connected to the borescope by a flexible light guide.

The borescope is inserted inside the glass tube fixed horizontally in the fluidized bed. The light from the light source is transmitted from the proximal to the distal end and illuminates the surface after being reflected from the mirror. The images of the illuminated particles on the glass tube surface and of the illuminated light guide ring are focused by objective lens *a* on the input face of image guide b_1. The latter transmits the image to the proximal end where relay lens c_1 in the eyepiece assembly magnifies it for viewing either directly or on a TV monitor, *h*, by means of closed-circuit TV camera *g*. The projected image is also recorded on a video cassette, *i*, for detailed analysis. The black-and-white TV camera has a C-mount lens, g_1, with a maximum aperture of $f/1.8$. The vidicon (image) tube in the camera converts optical images into synchronized electrical signals to be fed to the TV monitor, which has a resolution of 500 lines. Here the cathode ray tube converts the synchronized electrical signal into the optical image at the standard rate of 30 frames per second. An industrial Panasonic video cassette recorder (VCR), *i*, records this synchronized signal on a high-density Scotch Colorplus video cassette. There are four video heads in this VCR; two are used for normal playback and the other two are used for slow and still modes of operation.

The borescope is used to view and to record the particle concentrations around the glass tube surface at four positions: 0° or bottom (B), 90° or left (L), 180° or top (T), and 270° or right (R). The recordings are made for the fixed bed and for the fluidized bed at seven fluidizing air velocities in the range up to $1.1U_{mf}$. U_{mf} is the minimum fluidization velocity; gas velocities beyond $1.1U_{mf}$ are not possible to achieve in our present system. Typical still photographs of the recordings for the fixed bed and the fluidized bed ($1.1U_{mf}$) are shown in Figure 2 for all four borescope observation positions. TV monitor pictures are used to compute the bed voidage at the tube surface, ϵ_s.

In our discussion of the bed voidage at the tube surface, we consider only a region of 0.5 d_p thickness at the surface, ϵ_s is defined as:

$$\epsilon_s = 1 - F\frac{\text{Total area of particle images on TV screen}}{\text{Total area of TV screen}} \quad (1)$$

The correction factor *F* depends on the shape, size, and position of the particle relative to the tube surface. *F* is defined as the ratio of the volume of the spherical particle enclosed within a distance of particle radius from the tube surface to the volume of

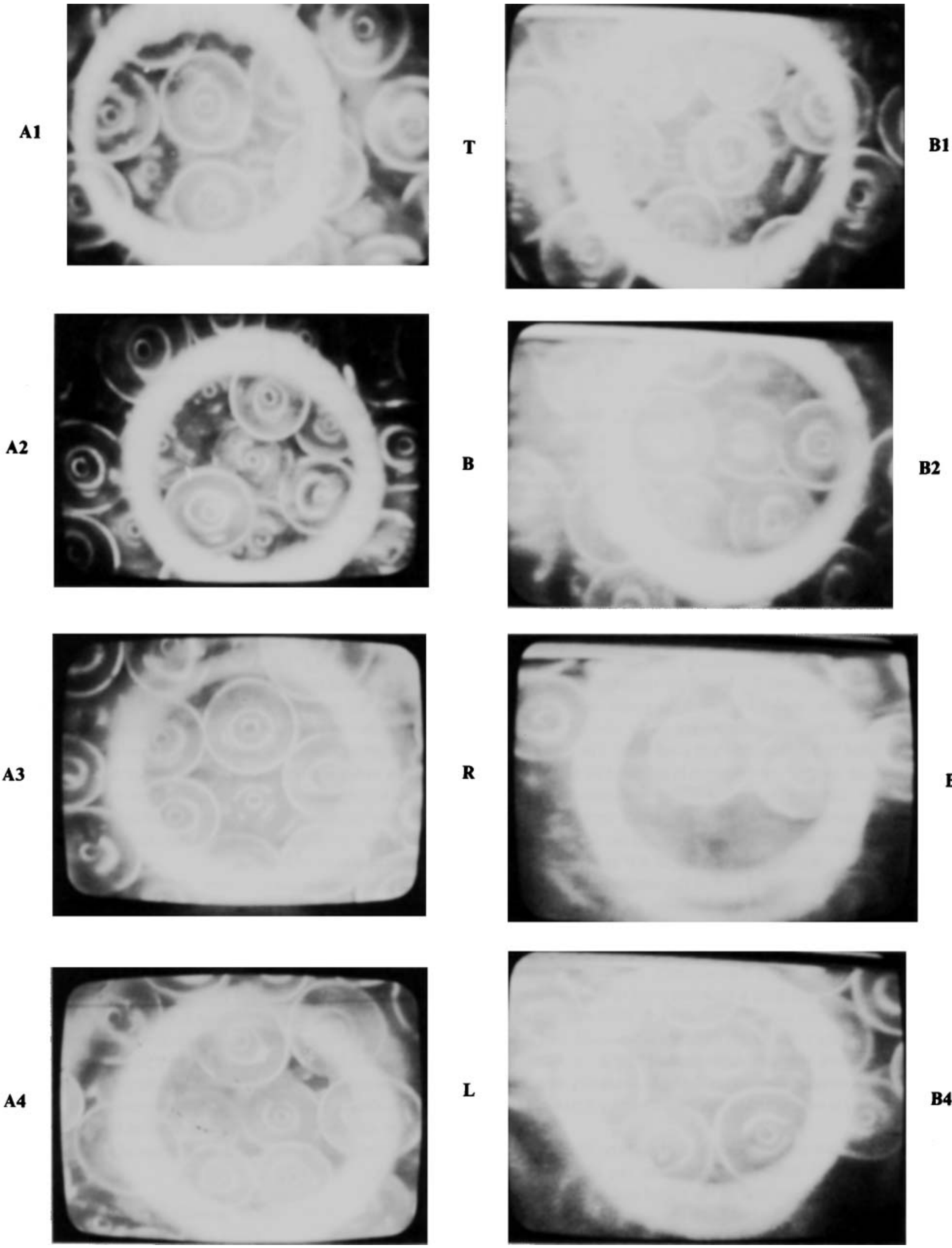

Figure 2. Still photographs at four positions.

A, fixed bed; B, fluidized bed
T = top; B = bottom; R = right; L = left

the cylindrical test section of diameter equal to the particle diameter and height equal to particle radius. For spherical particles, as is the case here, F is not dependent on d_p when the particles are located at the surface. Its magnitude is found to monotonically decrease as the particle distance from the tube surface is increased. For $d_p = 1.4$ mm, we find F to decrease as the particle distance from the tube surface is increased as follows:

Particle Dist., mm	F
0	0.666
0.1	0.571
0.2	0.475
0.3	0.380
0.4	0.286
0.5	0.190
0.6	0.095
0.7	0

In these calculations the curvature of the tube surface is neglected, however the calculations will be valid approximations as long as d_p is much smaller than the tube diameter. The small size range of the particles will also introduce some error in this calculation, although it will be compensated to some extent due to the use of mean particle diameter.

The image size of a particle and the magnification factor depend on the particle position relative to the tube surface, or upon the distance of the particle from a reference plane defined here as a horizontal plane passing through the probe axis. Experimentally, the magnification factors, A, are determined for particles of 1.4 and 1.7 mm dia. and located at various positions from 4.8 to 8.25 mm above this reference plane. The magnification factor uniquely depends on the particle position; it decreases as the distance increases and is independent of d_p.

Results

Typical records of the type shown in Figure 2A are employed to compute ϵ_s at the four positions (L, T, R, and B) around the tube for the fixed-bed configuration as well as to check the validity of the ϵ_s calculation procedure outlined above based on Eq. 1. The test section (5.5 × 4.0 mm) illuminated on the glass tube and viewed by the probe is analyzed on the TV monitor. The number of particles at each of these four positions is counted on the monitor screen and the actual surface voidage is computed assuming the particles to be spherical of radius 0.7 mm. Values of 0.642, 0.616, 0.628, and 0.628 for positions L, T, R, and B, respectively, are thus obtained. Three different video records for each position lead to ϵ_s values of 0.640, 0.615, 0.632 and 0.625 for the L, T, R, and B positions, respectively, based on Eq. 1 with $F = 0.667$. The two sets of values agree with each other within maximum and average deviations of 0.6 and 0.4%, respectively. This testifies to the accuracy of our procedure of calculation. Similar results for the fluidized bed are reported in Figure 3 for ϵ_s as a function of U/U_{mf}. Here U is the superficial gas velocity. Also shown in this figure is the bulk bed voidage, ϵ_b, obtained from pressure drop data across a region of 10 cm height below the tube. The following important conclusions are evident from these results.

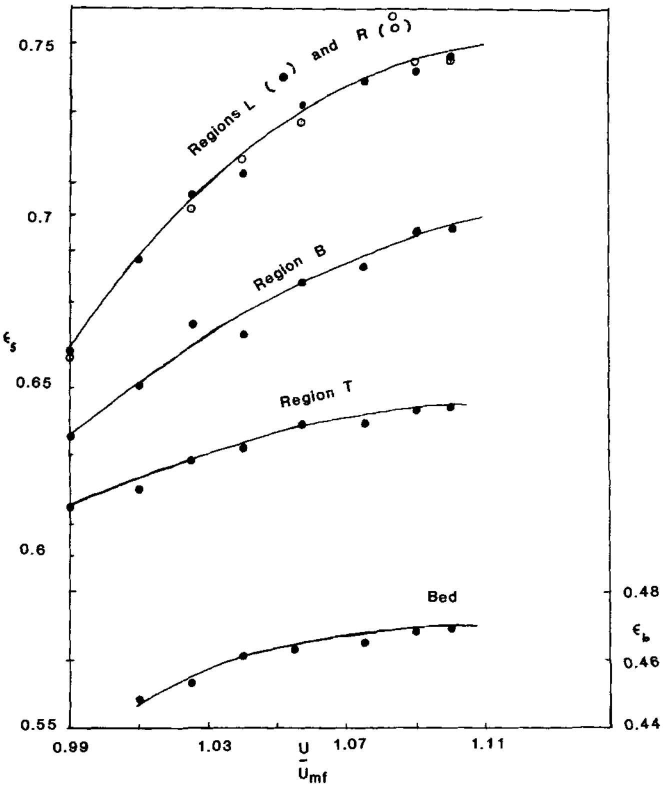

Figure 3. Variation of ϵ_s and ϵ_b as a function of U/U_{mf}.

The bed voidage in the vicinity of an immersed surface is different from that in the bulk of a fixed-bed configuration. The observed variation in ϵ_s around the surface of a circular tube, although not very significant, is still enough to warrant more detailed investigation. The proposed experimental technique is capable of measuring only the surface voidage, while the pressure probe technique is applicable for determining only the bulk bed voidage.

It is also clear from Figure 3 that the ϵ_s values for all four borescope observation positions and gas velocities are appreciably different from the ϵ_b values. The ϵ_s values for the L and R positions are approximately equal, and are larger than the values for the B and T positions. The ϵ_s values for the B position are larger than those for the T position. These qualitative results are in general agreement with the expected variations of ϵ_s inferred by several earlier workers. The present work provides a novel technique for directly determining these values in a three-dimensional system.

It is also noted that ϵ_s values are dependent on U, and the nature of variation depends upon the region under consideration around the periphery of the tube. Our measurements also provide details concerning the average particle distance from the tube surface at various angular positions and gas velocities. An average distance for most of the particles at positions B, L, and R for most of the time is 0.09 mm or 0.07 d_p. In this calculation the knowledge of the experimentally determined A values as a function of particle distance from the refernce plane is used. Detailed investigations with particles of different sizes and tubes of different diameters will reveal general quantitative trends for ϵ_s variation that could not be determined so far. Investigations of this nature are in progress and will be published in the future along with a comparison from somewhat similar results obtained at MIT using a capacitance probe.

Literature cited

Ishida, M., and H. Hatano, "The Behavior of Gas and Solid Particles in a Gas-Solid Fluidized Bed Detected by Optical Fiber Probes," *Fluidization,* D. Kunii and R. Toei, eds., Engineering Foundation, New York (1984).

Ishida, M., A. Nishiwaki, and T. Shirai, "Movement of Solid Particles around Bubbles in a Three-Dimensional Fluidized Bed at High Temperatures," *Fluidization,* J. R. Grace, and J. M. Matsen, eds., Plenum, New York (1980).

Kapany, N. S., *Fiber Optics—Principles and Applications,* Academic Press, New York (1967).

Louis, J. F., "Fiber Optic Sensor Fluidized-Bed Behavior Measurement," Rep. No. DOE/MC/16521-1339 (DE83005734), Nat. Tech. Info. Serv., U.S. Dept. Commerce, Springfield, VA (1982).

Peters, M. H., L. S. Fan, and T. L. Sweeney, "Study of Particle Ejections in the Freeboard Region of a Fluidized Bed with an Image-Carrying Probe," *Chem. Eng. Sci.,* **38,** 481 (1983).

Saxena, S. C., A. Mathur, and G. K. Sharma, "Bubble Dynamics and Elutriation Studies in Gas-Fluidized Beds," *Chem. Eng. Commun.,* **29,** 35 (1984).

Verma, R. S., and S. C. Saxena, "Heat Transfer from an Immersed Vertical Tube to a Gas-Fluidized Bed," *Energy,* **8,** 909 (1983).

Werther, J., and O. Molerus, "The Local Structure of Gas-Fluidized Beds. I: A Statistically Based Measuring System," *Int. J. Multiphase Flow,* **1,** 103 (1973).

Manuscript received Jan. 29, 1986, and revision received July 10, 1986.